4-Hydroxythiophenol-Protected Gold Nanoclusters in Aqueous Media

Shaowei Chen*

Department of Chemistry and Biochemistry, Southern Illinois University, Carbondale, Illinois 62901-4409

Gold nanoclusters protected by a monolayer of 4-hydroxythiophenol (HOPhSAu MPCs) were synthesized and characterized by various analytical techniques. The particles were found to be soluble in alkaline aqueous solutions, whereas at low pH, flocculation of particles started to occur. Acid/base titration of particle solutions indicated that the pK_a of particle-bound phenol moieties was close to 10, about 1 unit higher than that of free monomers (ca. 8.9). Transmission electron microscopy (TEM) was employed to measure the average particle size (ca. 5 nm) and size dispersity (ca. 30%), where the resulting size histograms exhibited two major populations centered around 6 and 4 nm. Upon decreasing solution pH, partial fractionation was effected, with smaller particles showing a higher solubility at lower pH. UV−vis spectroscopic measurements showed a surface-plasmon band at about 530 nm in various organic media. The red-shift of this band, relative to that of alkanethiolate or arenethiolate MPCs, might be due to particle flocculation as well as the electronic interactions between the phenyl moiety and the gold core that were facilitated by the hydroxy functional groups. In aqueous solutions, the surface-plasmon band position shows a slight red-shift with decreasing solution pH, and the absorption intensity monitored at this position exhibited a titration-like pH-dependent feature. A cyanide decomposition study of these particles showed a rather rapid rate constant, which might be ascribed to the enhanced partition of cyanide into the aromatic monolayers. Electrochemical studies of an aqueous solution of HOPhSAu particles and self-assembled monolayers of HOPhSH on a gold electrode surface both exhibited a pair of (quasi)reversible voltammetric waves, where the peak position shifted cathodically with increasing solution pH. A reaction mechanism was proposed which involved the formation of a carbonium intermediate in the electro-oxidation of the phenol moieties.

Introduction

Research interests in nanocrystals have been intensified lately, with a focus on the unique chemical, physical, and electronic properties associated with materials of these dimensions, as well as on their great application potentialities in diverse fields, such as electronic nanodevices, molecular catalysts, multifunctional reagents, and chemical sensors/biosensors.[1,2] Among these, monolayer-protected gold nanoclusters (MPCs), synthesized in a bi-phasic system,[3] have attracted particular attention, as these particles are stable in both solution and dry forms, in contrast to conventional colloidal particles.[2] There have been extensive research efforts devoted to the in-depth characterizations of these MPC materials,[3−6] in which the emphases have been on the experimental controls of particle size and size dispersity as well as on further functionalization of the particle monolayers, for instance, by surface coupling[7] or surface exchange reaction.[8,9] In addition, recent studies have shown that these particles behave as diffusive nanoelectrodes in solutions[8] and exhibit quantized electron-charging features with solutions of particles of relatively monodisperse core size, which have been found to be dependent both on the core size as well as on the monolayer structures.[10,11]

However, past studies have been mostly focused on particles passivated with alkanethiolate monolayers, likely due to the existence of extensive literature on self-assembled monolayers of alkanethiols on flat surfaces,[12,13] whereas there are only limited reports on studies of particles coated with monolayers containing aromatic moieties.[11,14] Recently, we reported on studies of gold

* Tel.: (618) 453-2895. Fax: (618) 453-6408. E-mail: schen@chem.siu.edu.

(1) (a) Schmid, G. *Clusters and Colloids: From Theory to Applications*; VCH: New York, 1994. (b) *Clusters of Atoms and Molecules*; Haberland, H., Ed.; Springer-Verlag: New York, 1994. (c) Turton, R. *The Quantum Dot: A Journey into the Future of Microelectronics*; Oxford University Press: New York, 1995.

(2) Hayat, M. A., Ed. *Colloidal Gold: Principles, Methods, and Applications*; Academic Press: New York, 1989; Vol. 1.

(3) Brust, M.; Walker, M.; Bethell, D.; Schiffrin, D. J.; Whyman, M. *J. Chem. Soc., Chem. Commun.* **1994**, 801.

(4) (a) Hostetler, M. J.; Murray, R. W. *Curr. Opin. Coll. Interface Sci.* **1997**, *2*, 42. (b) Hostetler, M. J.; Wingate, J. E.; Zhong, C.-J.; Harris, J. E.; Vachet, R. W.; Clark, M. R.; Londono, J. D.; Green, S. J.; Stokes, J. J.; Wignall, G. D.; Glish, G. L.; Porter, M. D.; Evans, N. D.; Murray, R. W. *Langmuir* **1998**, *14*, 17.

(5) Whetten, R. L.; Khoury, J. T.; Alvarez, M. M.; Murthy, S.; Vezmar, I.; Wang, Z. L.; Stephens, P. W.; Cleveland, C. L.; Luedtke, W. D.; Landman, U. *Adv. Mater.* **1996**, *8*, 428.

(6) Leff, D. V.; Ohara, P. C.; Heath, J. R.; Gelbert, W. M. *J. Phys. Chem.* **1995**, *99*, 7036.

(7) (a) Templeton, A. C.; Hostetler, M. J.; Warmoth, E. K.; Chen, S.; Hartshorn, C. M.; Krishnamurthy, V. M.; Forbes, M. D. E.; Murray, R. W. *J. Am. Chem. Soc.* **1998**, *120*, 4845. (b) Templeton, A. C.; Hostetler, M. J.; Kraft, C. T.; Murray, R. W. *J. Am. Chem. Soc.* **1998**, *120*, 1906.

(8) (a) Green, S. J.; Stokes, J. J.; Hostetler, M. J.; Pietron, J. J.; Murray, R. W. *J. Phys. Chem. B* **1997**, *101*, 2663. (b) Green, S. J.; Pietron, J. J.; Stokes, J. J.; Hostetler, M. J.; Vu, H.; Wuelfing, W. P.; Murray, R. W. *Langmuir* **1998**, *14*, 5612.

(9) Hostetler, M. J.; Green, S. J.; Stokes, J. J.; Murray, R. W. *J. Am. Chem. Soc.* **1996**, *118*, 4212.

(10) (a) Ingram, R. S.; Hostetler, M. J.; Murray, R. W.; Schaaff, T. G.; Khoury, J.; Whetten, R. L.; Bigioni, T. P.; Guthrie, D. K.; First, P. N. *J. Am. Chem. Soc.* **1997**, *119*, 9279. (b) Chen, S.; Ingram, R. S.; Hostetler, M. J.; Pietron, J. J.; Murray, R. W.; Schaaff, T. G.; Khoury, J. T.; Alvrez, M. M.; Whetten, R. L. *Science* **1998**, *280*, 2098. (c) Chen, S.; Murray, R. W.; Feldberg, S. W. *J. Phys. Chem. B* **1998**, *102*, 9898.

(11) Chen, S.; Murray, R. W. *Langmuir* **1999**, *15*, 682.

(12) Ulman, A. *An Introduction to Ultrathin Organic Films from Langmuir−Blodgett to Self-Assembly*; Academic Press: Boston, 1991.

(13) (a) Nuzzo, R. G.; Allara, D. L. *J. Am. Chem. Soc.* **1983**, *105*, 4481. (b) Li, T. T. T.; Weaver, M. J. *J. Am. Chem. Soc.* **1984**, *106*, 6107. (c) Bain, C. D.; Evall, J.; Whitesides, G. M. *J. Am. Chem. Soc.* **1989**, *111*, 7155. (d) Chidsey, C. E. D.; Loiascono, D. N. *Langmuir* **1990**, *6*, 682.

nanoparticles protected by a series of arenethiolate monolayers (with varying lengths of methylene spacers between the thiol and the aromatic ring),[11] where we found that there were quite significant effects of the ligand structures on the corresponding particle size and size dispersity, in contrast to the case of alkanethiolate MPCs. On the other hand, optical studies showed that the dielectric properties of the protecting aromatic monolayers remained virtually unchanged with varied alkyl spacers, whereas the vibrational spectroscopic studies suggested that there might be electronic interactions between the aromatic moieties and the gold cores as well as between neighboring aromatic ligands.

In this report, we carried out a series of studies of gold nanoparticles protected by 4-hydroxythiophenol monolayers (HOPhSAu). HOPhSAu MPCs have been synthesized by Schiffrin et al.[14a] by reducing gold (III) in a single-phase system (methanol) and were characterized by various spectroscopic techniques, which indicated that a protecting monolayer of hydroxythiophenol was formed on the gold particle surface and that further surface functionalization could be achieved by esterification of the particle-bound phenolic moieties.[14a] Our interests here, however, focus on investigating the effects of aromatic ring functionalization on the particle properties, for instance, optical responses, particle stability, and electrochemical charging behaviors. In addition, as these particles are soluble in (basic) aqueous media,[15] the charge state of the protecting ligands can be simply controlled by solution pH, thereby allowing us to compare the particle properties in varied media and to explore possible applications in biological systems.

Experimental Section

Chemicals. Sodium borohydride (99%, Aldrich), tetra-*n*-octylammonium bromide (Oct$_4$NBr, 98%, Aldrich), tri(hydroxymethyl)aminomethane (Tris, 99.9+%, Aldrich), potassium hydroxide (Acros), and hydrochloric acid (Fisher) were used as received. 4-Hydroxythiophenol (HOPhSH, 90%, Aldrich) and potassium nitrate (KNO$_3$, Fisher) were both recrystalized prior to use. Hydrogen tetrachloroaurate (from 99.999% pure gold) was synthesized using a literature procedure.[16] Water (>18 MΩ) was obtained with a Millipore Nanopure water system.

Synthesis. 4-Hydroxythiophenol-protected gold nanoparticles (HOPhSAu MPCs) were synthesized by a single-phase reduction reaction, similar to that described previously,[14a] except that 1 equiv of HOPhSH vs HAuCl$_4$ was used. The reaction solution was kept at ambient temperature. The resulting HOPhSAu MPCs were found to be very stable in the solvent-free form. Like short-chain alkanethiolate MPCs[4] and other arenethiolate MPCs,[11] they were powdery; however, they demonstrated very different solubility properties: not soluble in apolar organic solvents; very soluble in polar solvents (e.g., alcohols, acetone) and water at high pH (≥10). The clusters were rinsed thoroughly with diethyl ether to remove excessive HOPhSH ligands. The final cluster materials were found to be spectroscopically clean, as revealed by ^{1}H NMR (Varian VXR-500), where no sharp features associated with free thiols, disulfides or reaction byproducts were observed.

Spectroscopy. UV–vis spectra were acquired with an ATI Unicam-4 UV/Vis spectrometer (resolution 2 nm) with typically a 0.5 mg/mL MPC concentration in various organic solvents or in Nanopure water (pH buffered with Tris, KOH, and HCl) in a 1-cm quartz cuvette. The solution had been centrifuged at 3200

rpm for about 30 min to remove possible particle aggregates before being transferred to the cuvette for optical measurements. The data obtained were analyzed with a commercial program (VISION), in which the surface-plasmon band position was determined by the second-order derivative of the absorption spectra.

Transmission Electron Microscopy (TEM). TEM samples were prepared by spreading one drop of a ~1 mg/mL cluster aqueous solution (at various pHs) onto standard carbon-coated (20–30 nm) Formvar films on copper grids (600 mesh), drying in air for ca. 1 h. Phase contrast images of the particles were obtained with a side-entry Hitachi 7100 electron microscope operating at 100 keV. Three typical regions of each sample were imaged at 200K or 300K magnification. Size distributions of the gold cores were obtained from digitized photographic enlargements of at least 300 well-separated particles using Scion Image Beta Release 2 (available at www.scioncorp.com), in which values from twins or aggregates of particles were removed manually.

Acid/Base Titration. 4-HOPhSH and HOPhSAu MPCs were dissolved in 0.1 M KOH solutions, which were then back-titrated with 0.6 M HCl, monitored by a Corning 445 pH meter fitted with a standard glass/SCE combination electrode. The equivalent point was then detected from pH vs V_{HCl} plots.

Kinetics of MPC Decomposition by Cyanide. As shown previously,[7b] the rate at which monolayer-protected Au clusters are decomposed by cyanide provides a measure of core protection from this aggressive ligand. 1 mL of an aqueous solution of 2.6 mg HOPhSAu MPCs (final concentration ca. 3.2 μM in cluster and 13 mM in Au) was quickly mixed with 2 mL of an aqueous NaCN solution (final concentration ca. 6.5 mM). The decay in absorbance (at $\lambda = 540$ nm) was monitored over at least three reaction half-lives on an ATI Unicam-4 UV/vis spectrometer, as the dark blue cluster solution decomposed into one containing light brown/yellow, slightly soluble cyano-Au complexes (assumed, actual identity of Au product not determined), disulfides (~90% of the recovered organic matter), and aryl cyanides. The latter products were determined by ^{1}H NMR. The absorbance decay data were fit to a general first-order equation, $y = y_0 + ae^{-kt}$, where y is the experimental absorbance and y_0 is a constant term accounting for a small amount of absorbance and/or light scattering by the reaction product (i.e., loss of transmittance). More details are provided in the Results and Discussion section.

HOPhSH Monolayers. A gold electrode (area 0.076 cm^2) with self-assembled monolayers of HOPhSH was prepared by immersing a freshly cleaned gold electrode into a ca. 3 mM ethanolic solution of HOPhSH for at least 24 h. The electrode was then rinsed with copious ethanol and dried by nitrogen before being transferred into a 0.1 M KNO$_3$ solution for electrochemical measurements, where the solution pH was adjusted by a Tris–HCl buffer.

Electrochemistry. Electrochemical measurements were carried out with a BAS Model 100B/W Electrochemical Workstation. HOPhSAu MPC solution (ca. 64 μM) was prepared in 0.1 M KNO$_3$ with solution pH controlled by a Tris–HCl buffer. The electrodes were a glassy carbon disk working electrode (3.0 mm in diameter), a Ag/AgCl (3 M KCl) reference electrode, and a Pt coil counter electrode. The working electrode was polished with 0.05 μm Al$_2$O$_3$ (Buehler) slurries between experimental runs, followed by thorough rinsing with dilute H$_2$SO$_4$ solution and Nanopure water, consecutively. The cell solution was degassed for ca. 30 min with H$_2$O-saturated high purity N$_2$ prior to electrochemical measurements and blanketed with an N$_2$ atmosphere during the entire experiments.

Results and Discussion

In this section, we begin with a description of the solubility properties of HOPhSAu MPC obtained by simple pH titration, followed by further characterizations with TEM, UV–vis, and electrochemical techniques. Comparisons with alkanethiolate- and other arenethiolate-MPCs will also be discussed.

pH Titration. Acid/base titration of nanoparticles with ionizable monolayer moieties have been carried out previously, namely, in solutions of tiopronin and coenzyme A protected gold nanoparticles.[15a] The particle-bound acid

(14) (a) Brust, M.; Fink, J.; Bethell, D.; Schiffrin, D. J.; Kiely, C. *J. Chem. Soc., Chem. Commun.* **1995**, 1655. (b) Johnson, S. R.; Evans, S. D.; Mahon, S. W.; Ulman, A. *Langmuir* **1997**, *13*, 51.

(15) (a) Templeton, A. C.; Chen, S.; Gross, S. M.; Murray, R. W. *Langmuir* **1999**, *15*, 66. (b) Schaaff, T. G.; Knight, G.; Shafigullin, M. N.; Borkman, R. F.; Whetten, R. L. *J. Phys. Chem. B* **1998**, *102*, 10643.

(16) *Handbook of Preparative Inorganic Chemistry*; Brauer, G., Ed.; Academic Press: New York, 1965.
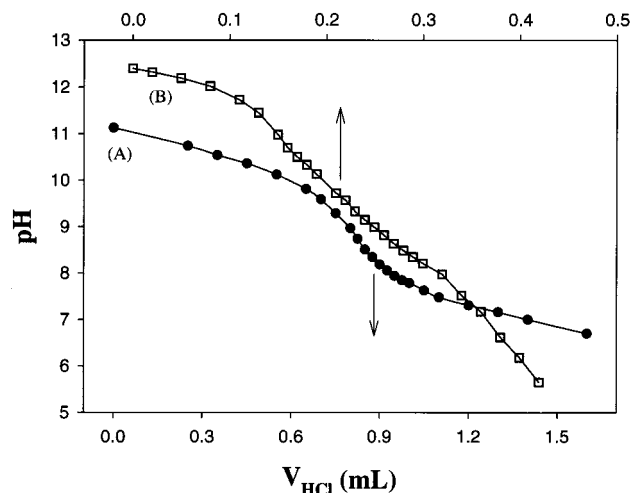
Figure 1. pH titration of (A) 4-HOPhSH and (B) HOPhSAu MPCs. Free monomers and MPCs were first dissolved in 0.1 M KOH, then back-titrated with 0.6 M HCl. 4-HOPhSH initial concentration, 0.065 M. HOPhSAu MPCs initial concentration, ca. 10 μM.

moieties exhibited a pK_a 1 to 2 units higher than that of the corresponding monomers, which was attributed to the electrostatic interactions between neighboring ligands in the monolayers.[15a] Figure 1A shows the titration curve for the monomer HOPhSH, in which a sharp equivalent point can be found at pH around 8.9. For HOPhSAu MPCs, however, the equivalent point is not as well-defined (Figure 1B), and it appears that the pK_a lies close to 10, corresponding to an increase of ca. 1 unit compared to that of the free monomer; again, most likely resulting from the interactions between neighboring monolayer ligands.

It should be noted that the particles exhibited good solubility at high pH (>11), whereas at low pH (<10), flocculation of particles started to occur. This could be partially attributed to the interparticle interactions. Arenethiolate MPCs have been found to exhibit greater interparticle interactions than their alkanethiolate counterparts, presumably due to the π-electron-rich phenyl moieties.[11] For HOPhSAu MPCs, at low pH, the hydroxy functional groups further facilitate interparticle interactions, possibly through an H-bonding network, resulting in the formation of particle aggregates. Such a behavior has also been observed with carboxylate-stabilized particles at low pH.[17] However, at high pH, particle aggregation is less likely to occur due to the repulsive interaction between negatively charged particles.

Transmission Electron Microscopy (TEM). There has been extensive work in using TEM to characterize particle size[4] as well as particle superlattice structures.[18] In combination with results from other analytical techniques, it has been postulated that the most likely geometric shape of these gold MPCs is a truncated decahedron (TD) or truncated octahedron (TO).[19] Figure 2 shows two representative TEM micrographs of HOPhSAu MPCs deposited from a basic aqueous solution at pH = 13.20 and 8.95, with the size distributions shown in the insets. The common feature is that small particle aggregates can be seen even at high pH, most likely due to

strong interparticle interaction or electron-beam damage of particles.[11] On the other hand, chains of particles can be found, akin to the observations with arenethiolate-MPCs,[11] which have been interpreted based on the self-assembling of particles into bilayer-like structures with the top layer sitting on the 2-fold saddle rather than the 3-fold hollow sites. These bilayer-like structures are probably due to the balance of electrostatic repulsion and dispersion interactions between neighboring particles.[11]

The average particle size from this specific synthetic condition is about 5 nm, with a dispersity of about 1.5 nm (30%; Figure 2A inset). The particles are much bigger than previously studied alkanethiolate-[4] and arenethiolate-MPCs[11] synthesized in a bi-phasic system at the same thiol/gold ratio and solution temperature. Assuming a TO configuration of the gold core, this corresponds to a composition of about 2951−4033 gold atoms.[4] At high pH (= 13.20, Figure 2A inset), there appears to be two major populations centered at 4 and 6 nm, respectively. At lower solution pH (<12, Figure 2B inset), the population at 6 nm disappears, and the dominant population is centered at 4 nm. As the size distribution was measured from well-separated particles (i.e., excluding patches and chains), the diminishing of the bigger particles can be attributed to the size dependency of particle solubility at various solution pHs.

This pH-gated fractionation might be a general route to easy separation of particles according to their core size if the particle charged state can be readily controlled by solution pH. This method is similar to the previous separation method using a solvent−nonsolvent (i.e., apolar−polar) mixture for alkanethiolate and arenethiolate MPCs, both of which take advantage of the particle property of size-sensitive solubility.[20]

UV−Vis Spectroscopy. Particles on the nanoscale exhibit unique optical properties, in which the typical feature includes an exponential decay of the absorption spectra with increasing wavelength (Mie scattering) onto which a surface-plasmon (SP) band is superimposed. The specific SP energy (wavelength) of nanoparticles has been found to be extremely sensitive to the particle size and shape as well as to the optical and electronic properties of the immediate surrounding media.[21] Previous studies have shown that organic-monolayer-protected gold nanoclusters also exhibit a characteristic surface-plasmon band, due to the interband transition of the gold core 5d electrons,[21,22] that is virtually independent of solvent media.[4] Figure 3A shows the UV−vis spectrum of HOPhSAu MPCs in various organic media, where a rather visible surface-plasmon band (±2 nm) can be found at 530 nm in alcohol and THF and in a slightly different position in acetone, 525 nm. A similar surface-plasmon feature can also be seen in aqueous solutions at varied solution pH, at approximately the same energy (530 nm; Figure 3B). Earlier studies showed that gold MPCs (diameter ≤ 5 nm) with alkanethiolate[4b,21,22] or arenethiolate monolayers[11] in organic media, gold MPCs with biological thiol monolayers in aqueous solutions,[15] and much bigger "naked" gold colloidal particles (5−10 nm)[2] all exhibited a surface-plasmon band at about 520 nm. The quite

(17) Chen, S.; Kimura, K. *Langmuir* **1999**, *15*, 1075.

(18) (a) Harfenist, S. A.; Wang, Z. L.; Alvarez, M. M.; Vezmar, I.; Whetten, R. L. *J. Phys. Chem.* **1996**, *100*, 13904. (b) Wang, Z. L.; Harfenist, S. A.; Whetten, R. L.; Bentley, J.; Evans, N. D. *J. Phys. Chem. B* **1998**, *102*, 3068.

(19) Cleveland, C. L.; Landman, U.; Schaaff, T. G.; Shafigullin, M. N.; Stephens, P. W.; Whetten, R. L. *Phys. Rev. Lett.* **1997**, *79*, 1873.

(20) Schaaff, T. G.; Shafigullin, M. N.; Khoury, J. T.; Vezmar, I.; Whetten, R. L.; Cullen, W. G.; First, P. N.; Gutiérrez-Wing, C.; Ascensio, J.; Jose-Yacamán, M. J. *J. Phys. Chem. B* **1997**, *101*, 7885.
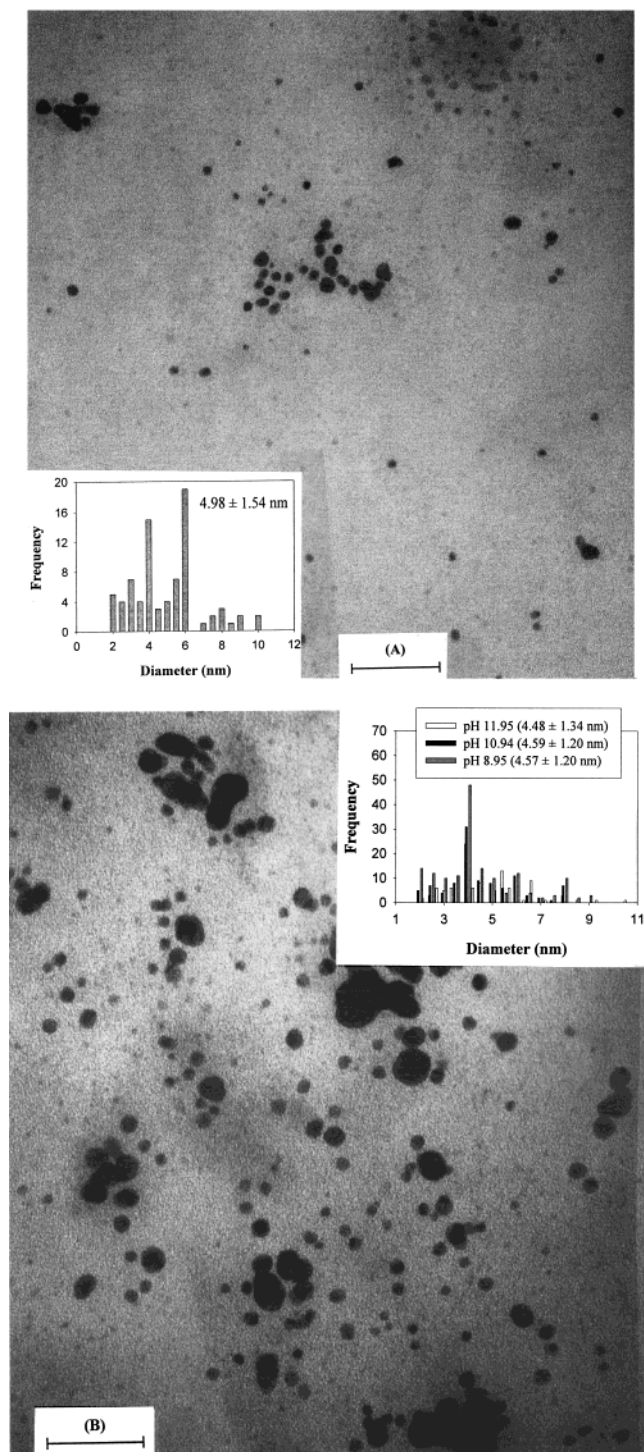
(21) (a) Kerker, M. *The Scattering of Light and Other Electromagnetic Radiation*; Academic Press: New York, 1969. (b) Bohren, C. F.; Huffman, D. R. *Absorption and Scattering of Light by Small Particles*; John Wiley & Son: New York, 1983; Chapter 12. (c) Underwood, S.; Mulvaney, P. *Langmuir* **1994**, *10*, 3427. (d) Mulvaney, P. *Langmuir* **1996**, *12*, 788.

(22) Alvarez, M. M.; Khoury, J. T.; Schaaff, T. G.; Shafigullin, M. N.; Vezmar, I.; Whetten, R. L. *J. Phys. Chem. B* **1997**, *101*, 3706.

Figure 2. Transmission electron micrographs of HOPhSAu MPCs cast from solutions at various pHs: (A) 13.20; (B) 8.95. Scale bars in (A) and (B) are 50 and 33 nm, respectively. Insets depict the corresponding core size histograms with average core sizes shown in the figure legends.

significant red-shift observed here with HOPhSAu particles in various media might be accounted for by various sources, for instance, (i) effects of monolayer functionalization on the dielectric properties of the protecting layers[11] and (ii) particle flocculation.

Monolayer functionalization on nanoparticle optical properties has been observed with gold colloidal particles in a hydrosol that was capped by 4-carboxythiophenol monolayers, where the surface-plasmon band energy shifted from 525 nm (uncapped) to 533 nm (capped).[23]

Therefore, the optical properties observed here with HOPhSAu MPCs could be, in part, due to the specific functional (hydroxy) groups of the protecting mercaptophenol adlayers. Further study of the effects of monolayer structures on particle electronic properties is desired to address this problem more specifically.

On the other hand, particle aggregation has been observed to account for the red-shifting and broadening of gold nanoparticle surface-plasmon resonance, which was attributed to the coupling of plasma modes between neighboring particles.[11,21] For instance, a red-shift (longer wavelength) of SP energy was found with decreasing solution pH in aqueous solutions of gold particles protected with tiopronin and coenzyme-A monolayers,[15a] a behavior that was most likely due to the formation of particle aggregates at low pH. Therefore, the observed SP red-shift of HOPhSAu MPCs relative to those of alkanethiolate-[4] or arenethiolate-MPCs[11] or colloidal gold[2] might, in part, be attributed to particle flocculation. Indeed, from Figure 3B, the surface-plasmon band position of HOPhSAu MPCs, as determined by the second-order derivative of the absorption spectra, demonstrates a slight shift to longer wavelength (lower energy) with decreasing solution pH: from 524 nm at pH = 13.2 to 534 nm at pH = 11.95 and to 530 nm at pH = 10.94. Solution absorbance at pH < 9.9 is too low to have a well-defined surface-plasmon band feature due to poor solubility of particles. As particle aggregates are formed at lower pH, for instance, by H-bonding networking between particles (as mentioned earlier) this observation appears to be consistent with the above argument.

Figure 3B, inset, shows the variation of solution absorbance at 530 nm with solution pH, where one can see that at pH ≥11, the absorbance is almost invariant, whereas at lower pH, the absorbance decreases sharply. As solution pH decreases, particles start to aggregate (indeed, particle precipitates are quite visible on the bottom of the cuvette), and consequently, the solution concentration decreases accordingly, consistent with the above titration study.

Cyanide Decomposition. MPC stability has been characterized by using a cyanide decomposition reaction, where it has been found that the reaction is first-order in both the concentrations of the clusters and the cyanide in solutions.[7b] As cyanide decomposes MPCs into colorless or slightly colored species, the reaction kinetics can be monitored easily by optical methods, and the decay of the absorbance can be fit with a general equation of $y = y_0 + ae^{-kt}$ where y_0 is the residual absorbance, a is the absorbance associated with particles, and k is the reaction rate constant (with excessive cyanide in solution, the overall reaction is pseudo-first-order). Figure 4 shows the decay of solution absorbance at 540 nm; in which one can see that it can be fitted very well with this exponential equation, from which the reaction rate constant can be evaluated. The rate constant (2.44 ± 0.02 M^{-1} s^{-1}) was found to be greater than those obtained with particles protected by alkanethiolates ($0.1 \sim 1$ M^{-1} s^{-1})[7b] and even greater than those with arenethiolate ($0.6-1.5$ M^{-1} s^{-1}, PhC2SAu; PhC4SAu; 4-CresolSAu; 2-NapSAu) monolayers,[11] suggesting that the phenyl functionalization (−OH) might facilitate cyanide partition into the monolayers, probably by the enhanced interactions between the π-electron-rich phenyl moiety and cyanide ions.

Reaction kinetics measured at varied wavelength positions show similar rate constants (data not shown), within experimental errors, and the nonzero residual absorbance

(23) Mayya, K. S.; Patil, V.; Sastry, M. *Langmuir* **1997**, *13*, 3944.
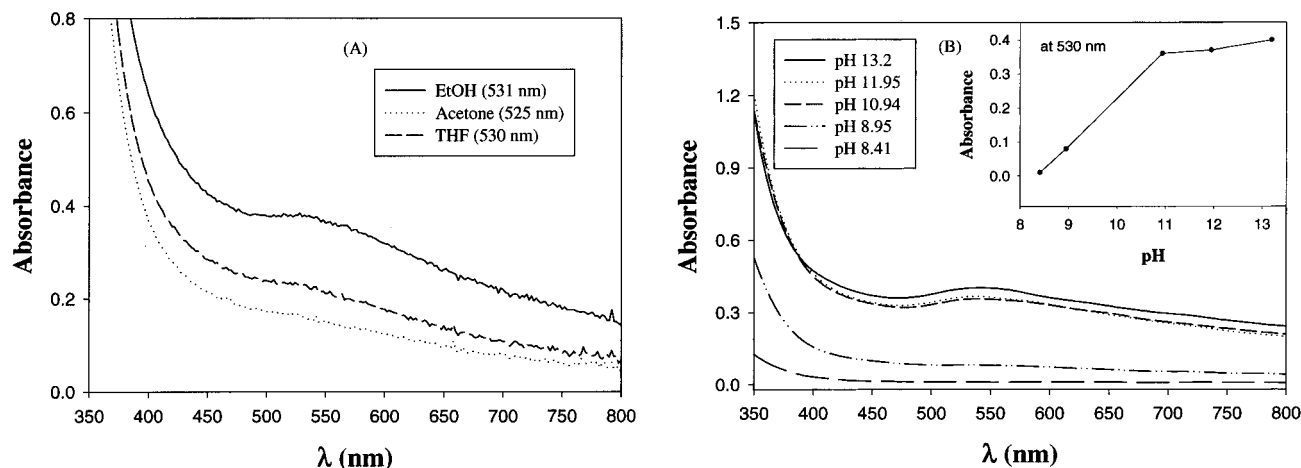
Figure 3. (A) UV−vis spectra of HOPhSAu MPC in various media: MPC concentration ca. 0.5 mg/mL, with corresponding surface-plasmon band positions shown in the figure legends. (B) UV−vis spectra of HOPhSAu MPC solutions at various pHs. Inset shows the variation of solution absorbance at 530 nm. Initial MPC concentration at pH = 13.20 ca. 0.5 mg/mL; solution pH buffered with 35 mM Tris, KOH, and HCl.
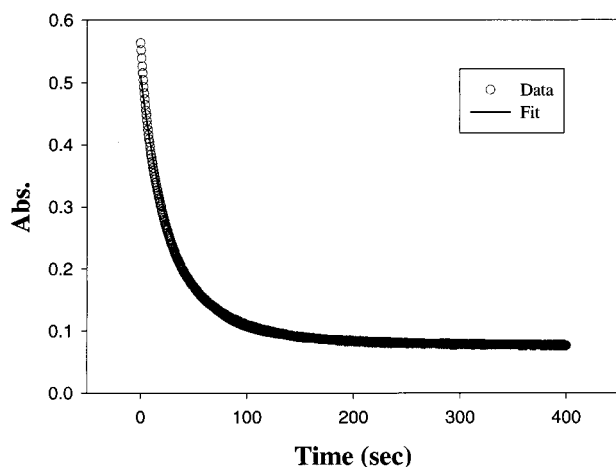
Figure 4. Kinetics of CN decomposition of HOPhSAu MPC measured by UV−vis spectrometry monitored at 540 nm. Symbols are the experimental data, and line is the exponential fit. MPC concentration, ca. 0.9 mg/mL, CN^- concentration, 6.5 mM; solution pH buffered with Tris, KOH, and HAc (pH ca. 13.20).

might be due to the absorption and/or scattering of the reaction products. These have been consistent with earlier studies.[7b,11]

Electrochemical Study. An electrochemical study of self-assembled monolayers of 4-hydroxythiophenol on flat gold surfaces exhibited a pair of voltammetric waves, in which the formal potential shifted cathodically with increasing solution pH (Figure 5). From the cyclic voltammograms (A, CV) and differential pulse voltammograms (B, DPV), one can see that the peak splitting between the anodic and cathodic scans ($\Delta E_p = E_{p,a} - E_{p,c}$) was typically less than 40 mV, suggesting a (quasi-)reversible electron-transfer process. In addition, the peak current was proportional to the potential scan rate (not shown), indicating that the electrochemical responses were due to surface-adsorbed species. However, to the best of our knowledge, no report about the exact reaction mechanism of the electron-transfer process involved has appeared.[24] In the voltammetric studies of the electro-oxidation of 4-methoxyphenol to quinone, Leedy proposed a two-electron, two-proton reaction mechanism involving
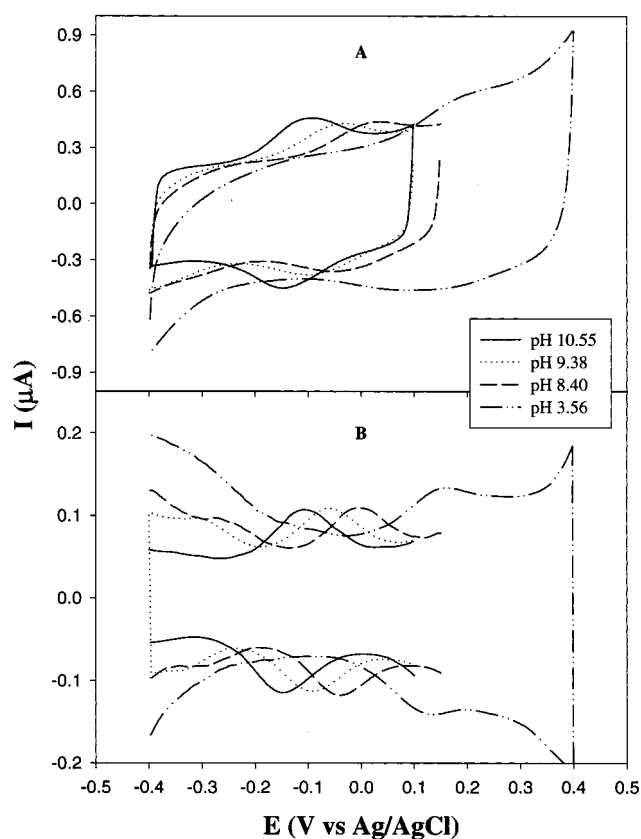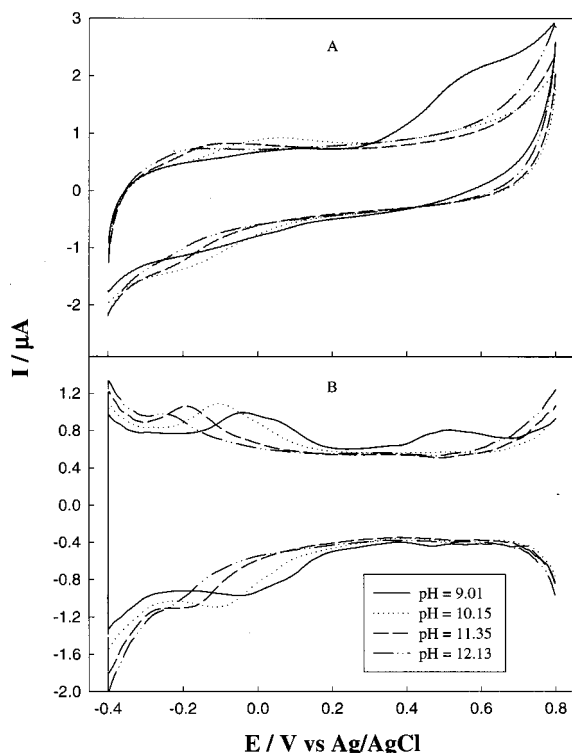

Figure 5. Cyclic voltammogram (A) and differential pulse voltammograms (B) of self-assembled monolayers of HOPhSH on a gold electrode surface in 0.1 M KNO_3 at various solution pHs buffered by 0.01 M Tris and HCl. (A) Potential sweep rate 100 mV/s; (B) Sweep rate 10 mV/s, pulse amplitude 50 mV, pulse width 200 ms.

formation of carbonium ions as the intermediates, which, in the presence of nucleophilic reagents, could then be trapped to form more complicated aromatic derivatives.[25] It is, therefore, suspected that hydroxythiophenol might follow a similar pathway (Scheme 1), giving rise to the observed voltammetric features. Furthermore, it is an-

(24) Hayes, W. A.; Shannon, C. *Langmuir* **1996**, *12*, 3688.

(25) Leedy, D. W. *Electroanal. Chem. Interfacial Electrochem.* **1973**, *45*, 467.

Figure 6. Cyclic voltammogram (A) and differential pulse voltammograms (B) of ca. 64 μM solutions of HOPhSAu MPCs in 0.1 M KNO$_3$ at various solution pHs buffered by 0.01 M Tris and HCl at a glassy carbon electrode (3.0 mm in diameter). (A) Potential sweep rate 500 mV/s; (B) Sweep rate 10 mV/s, pulse amplitude 50 mV, pulse width 200 ms.

Scheme 1 . Proposed Reaction Mechanism of 4-Hydroxythiophenol Immobilized on Gold Surfaces
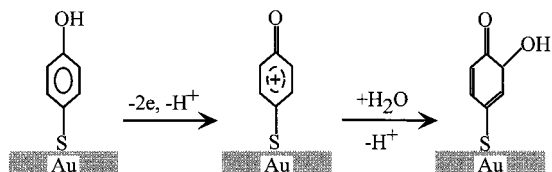
ticipated that similar responses will be observed with HOPhSAu MPC solutions. Figure 6 shows the cyclic voltammograms (A, CV) and differential pulse voltammograms (B, DPV) of HOPhSAu MPCs in an aqueous KNO$_3$ solution at various solution pHs, in which a pair of well-defined waves are better demonstrated by DPV. The peak positions and peak splitting are consistent with those observed with HOPhSH monolayers (Figure 5). In addition, the formal potential is also found to shift to more negative positions with increasing solution pH. On the basis of the proposed mechanism (Scheme 1), at room temperature, one should expect a ca. 54 mV cathodic shift of the formal potential with a one unit increase of solution pH. Figure 7 shows the pH dependency of the formal potentials; the linearity is quite good for both the monolayer and the MPC cases. However, the slopes are somewhat different from the predicted value, with a slope of about −48 and −62 mV per pH unit for the monolayer and MPC cases, respectively. The origin of this discrepancy is somewhat unclear; one possibility might be the structural effect of the phenol adlayers (i.e., 2D vs 3D) on the interactions between neighboring ligands and hence the nucleophilic attack by solution hydroxy moieties.

One might note that quantized capacitance charging was not observed here, despite the somewhat narrowed
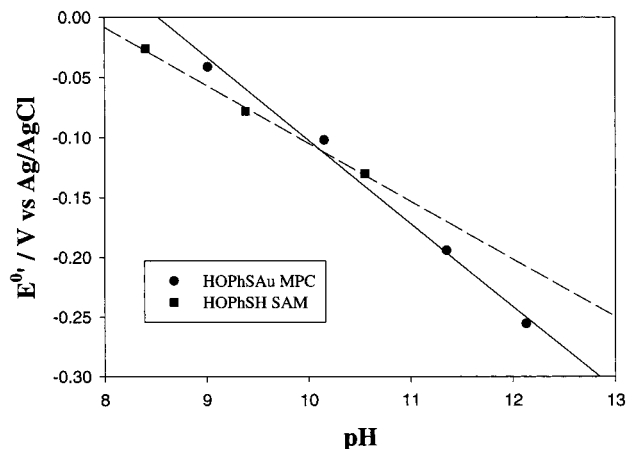
Figure 7. Variation of formal potentials with solution pH. Data obtained from Figures 5 and 6.

particle dispersity, which might be due mainly to the fact that the particle capacitance (C_{CLU}) is too big, and hence the small potential difference between consecutive charging steps ($\Delta V = e/C_{CLU}$, e is the electronic charge) is hard to detect, as predicted by theoretical analysis.[10c] On the other hand, kinetic effects might also play an important role, as electron-transfer energy barriers will be quite big due to the negatively charged monolayer structure. More study on this end is currently underway.

Concluding Remarks

Gold nanoparticles protected by 4-hydroxythiophenol monolayers have been prepared and studied. Solution pH titration indicates that (i) the particles are very soluble at high pH ($\geq$10); (ii) at lower pH (<10), particle flocculation starts to occur; and (iii) the pK_a for the surface-bound phenol groups lies approximately at 10, about 1 unit greater than that for the free monomers. The core size and size dispersity were characterized by a transmission electron microscopic technique; at pH > 13, two major populations were found at around 4 and 6 nm, whereas at lower pH (<12), the dominant population was centered at 4 nm. The diminishing of the bigger core-size particles was attributed to the pH-gated particle solubility, akin to a previously employed fractionation method using solvent–nonsolvent mixtures. In addition, TEM measurements revealed the formation of chains and patches of particles, which were accounted for by the strong interparticle interactions.

The UV–vis spectroscopic study exhibited a well-defined surface-plasmon band at about 530 nm in various organic media. In aqueous solution, the surface-plasmon band position was found to be slightly dependent on solution pH, where a shift to longer wavelength was observed with decreasing pH. On the other hand, the optical absorption property was utilized to monitor the reaction kinetics of nanoparticle decomposition by cyanide; the rate constant obtained was comparable to those found with other arenethiolate monolayers but much greater than those with alkanethiolate monolayers, probably due to the enhanced partitioning of cyanide into the monolayers.

Electrochemical studies of aqueous solutions of these MPCs showed a pair of (quasi)reversible waves, in which the peak potential was found to shift to more negative positions with increasing solution pH. These observations were consistent with those of a self-assembled monolayer of 4-hydroxythiophenol on a gold electrode surface. A

reaction mechanism involving the formation of a carbonium intermediate was proposed to account for these voltammetric responses.

A further and more comprehensive study is desired, especially in terms of the investigations of the effects of synthetic conditions, particle size, and dispersity on their optical and electrochemical properties.